Available online at www.sciencedirect.com
ScienceDirect
Trans. Nonferrous Met. Soc. China 20(2010) 1663−1671
Transactions of Nonferrous Metals Society of China
www.tnmsc.cn

Microstructural evolution during semisolid state strain induced melt activation process of aluminum 7075 alloy

A. BOLOURI[1], M. SHAHMIRI[2], E. N. H. CHESHMEH[2]

1. Department of Mechanical Engineering, Eastern Mediterranean University, Mersin 10, Turkey;
2. School of Material Engineering and Metallurgy, Iran University of Science and Technology, Tehran, 16844, Iran

Received 13 May 2010; accepted 25 June 2010

Abstract: The effects of compression ratio on the microstructure evolution of semisolid 7075 Al alloy produced by the strain induced melt activation (SIMA) process were investigated. The samples were cold deformed by compression into the different heights up to 40% reduction. The isothermal holding treatments were carried out at 625 °C for predetermined time intervals. The results reveal that the average grain size is gradually reduced with the increase of the compression ratio. When the compression ratio surpasses 30%, the above descending trend is not as evident as that below 30% reduction. During the subsequent heat treatments, the recrystallization is induced in the deformed samples by the increasingly accumulated strain energy. The grain growth mechanisms and the microstructural coarsening of the SIMA processed 7075 Al alloy were discussed and confirmed.
Key words: thixoforming; thermomechanical processing; aluminium alloys; semi-solid metal

1 Introduction

Semisolid metal (SSM) processing has been recognized as a technique offering several potential advantages over casting or solid state forming, such as producing high quality components capable of full heat treatment to maximize properties, and reducing macrosegregation, solidification shrinkage and forming temperature. Several reviews are available[1−4]. The key feature that permits the shaping of alloys in the semisolid state is the absence of dendritic characteristics from the morphology of the solid phase[5].

There are various types of semisolid processing [3−4]. Rheocasting refers to the process where the alloy is cooled into the semisolid state and injected into a die without an intermediate solidification step. Rheomoulding is allied to polymer injection moulding, and uses either a single screw or a twin screw. Thixo usually refers to processes where an intermediate solidification step does occur. There are exceptions to this, e.g. Thixomolding, which is used to produce magnesium alloy components, e.g. for portable computers and cameras. Thixoforming can cover both thixocasting, thixoforging and an intermediate process called thixoforming. Thixocasting tends to take place with relatively high fractions of liquid and thixoforging tends to happen when the fractions are lower.

The way to obtain semisolid slurries is the key to semisolid processing. Except for mechanical and magnetohydrodynamic stirring[6−8], strain induced melting activation (SIMA) process[9−10] is the most promising technology for preparing semisolid slurries, because it is simpler and has less requirements for equipment than stirring method. Meanwhile, more homogeneous and finer equiaxed microstructure can be obtained by SIMA process[11]. The SIMA process includes several steps. 1) Cold deformation or quenching of a hot extruded or rolled bar occurs to induce sufficient strain; 2) The billet is heated to a temperature between solidus and liquidus, and then kept isothermally for a certain period. In this step, following partial remelting, an extremely fine, uniform and non-dendritic spherical microstructure is generated. 3) The semisolid slurry with equiaxed grains is thixocast or thixoformed. In the whole process, only one part of the alloy is melted. Therefore, the atmosphere protection adopted in the normal casting process can be absent.

The net shape thixoforming of wrought alloys such as 7075[12−16] is of significant practical interest because these alloys are often shaped by extensively

Corresponding author: A. BOLOURI; Tel: +90-533-834-3349; E-mail: amir.bolouri@yahoo.com
DOI: 10.1016/S1003-6326(09)60355-1

costly machining of wrought material with much wastage. Understanding of the development of the spheroidal microstructure in the semi-solid state will enable optimisation for the practical application. In the present investigation, the effects of predeformation rate, as well as holding time and temperature at semisolid state on the microstructural characteristics of 7075 aluminum alloy specimens were investigated.

2 Experimental

The commercially pure starting material, within the 7075 specification (Table 1), was used in this work. The liquid fraction−temperature relationship was determined using differential scanning calorimetry (DSC). Samples of about 5 mm in diameter and 20 mg in mass were cut, weighed and put into carbon pans with carbon lids in an argon atmosphere. The DSC tests were carried out using a Dupont 910 differential scanning calorimeter. The samples were heated to 680 °C at 10 °C/min and cooled to room temperature at the same rate. The heat flow and temperature were monitored by thermocouples to obtain heating and cooling curves. The fraction liquid versus temperature curve was obtained by integrating under the curves.

Table 1 Composition of starting material (mass fraction, %)

Zn	Mg	Cu	Cr	Mn	Fe	Al
5.1−6.1	2.1−2.9	1.2−2.0	0.18−0.28	0.3	0.5	Bal.

Cylindrical samples, 31 mm in diameter and 34 mm in height, were machined from the starting material and were heated to 470 °C for 60 min to relieve the previous forming stresses and finally cooled in the air. These cylindrical samples were cold deformed by compression up to a height reduction of 40%. After cold compression, all samples were machined again to 20 mm in diameter (and same height for all reductions) to have homogenous strain in the core. A hole of 1.6 mm in diameter was drilled into the centre of each sample in order to insert a thermocouple for monitoring the temperature of the samples. Then, the samples were heated in a resistance heating furnace for predetermined time (up to 60 min) and temperature (with the mushy zone). Heating cycles were interrupted at various stages, samples were quenched and their microstructure was examined. Samples were ground up to 2 500 grit paper and polished down to 0.25 μm diamond paste. They were then etched using Keller solution.

Optical micrographs of the samples were taken using a UNION VERSAMET 3 equipped with OLYMPUS E300 digital camera, and the liquid fraction was estimated for each heat treatment. This was performed using image analysis (quantitative measurements), by measuring the volume fraction of the primary α(Al) phase particles, within the quenched liquid. All quantitative measurements were carried out using CLEMEX PROFESSIONAL EDTION software.

3 Results and discussion

3.1 Liquid fraction versus temperature

A curve for liquid fraction versus temperature derived from the DSC result is shown in Fig.1. It should be noted that the liquid content present in the micrographs is not the true quantity present at each temperature as the quench was not rapid enough for the liquid content to be entirely ‘frozen in’. During the quenching experiments, some liquid phase deposited onto the existing solid surfaces, appearing to be ‘solid’ in the quenched microstructure[17].

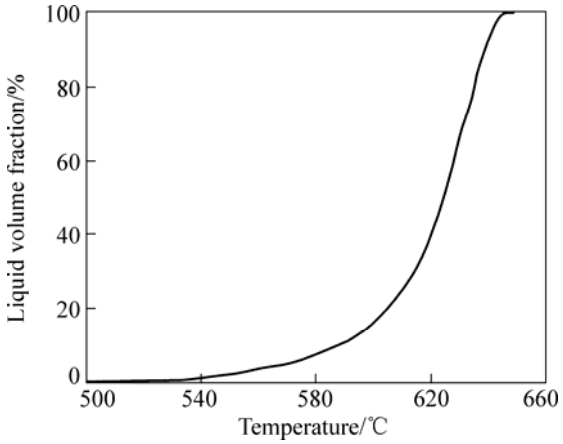

Fig.1 Liquid fraction vs temperature curve estimated from DSC heating curves

3.2 Effect of compression ratio on microstructure during partial remelting

An optical micrograph for the as-received 7075 aluminum alloy is shown in Fig.2. The microstructure consisted of unrecrystallised grains with various small dispersed particles, which are characteristics of such

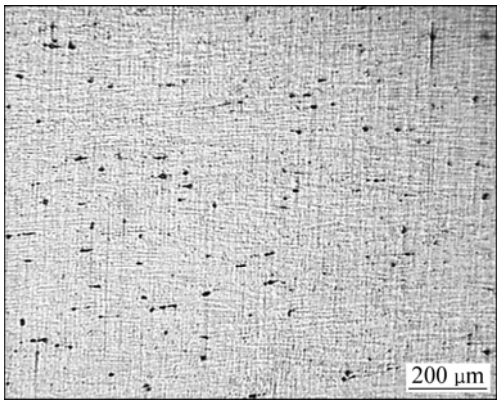

Fig.2 Optical micrograph for as-received 7075 aluminum alloy

alloys. Fig.3 shows the microstructures of as-deformed alloys with different compression ratios (10%, 15%, 20%, 30% and 40%) after isothermal holding at 625 °C for 5 min.

As shown in Fig.3, in general, grains were refined and more homogenous as the compression ratio increased. During compression of the alloys, dislocation density increases due to internal crystal lattice distortion. The increase in compression ratio leads to increase in distortion and internal strain energy, which is stored in the forms of vacancies, lattice defect and dislocation multiplication. We suppose that the recrystallisation is the main mechanism in breaking up the microstructure in SIMA process. Distortion energy will provide the driving force for recovery and recrystallisation during heating below solidus temperature. So during recovery, sufficient thermal energy is supplied to allow the dislocations to rearrange themselves into lower energy configurations, which occurs near melting point. After that, the residual distortion energy stored in the alloys provides the driving force for recrystallisation. This process consists of the replacement of grains containing high concentrations of dislocations with new grains containing much lower dislocation densities. It has been shown that, when the misorientation of such subgrains is larger than a critical angle, i.e. 20° in aluminum, the solid/liquid interface energy γ_{SL} becomes less than half of grain boundary surface energy γ_{gb}. When this condition is satisfied ($\gamma_{gb}>2\gamma_{SL}$), liquid penetrates the grain boundary, minimizing the local surface energy. Solid particles, whose grain boundaries are not wetted, become interconnected by coalescence and form agglomerates[18].

As shown in Fig.3(a), when the compression ratio was 10%, the microstructure consisted of some elongated solid particles, meaning that the microstructure breaking up mechanism is not active or effectively active. Microstructural comparison of samples with 10%, 15% and 20% compression ratios may identify the critical compression ratio at which the microstructures have relatively homogenous and refined grains. The microstructure of sample with 15% compression ratio mostly consisted of elongated grains but grains of the sample with 20% compression ratio were refined and acceptably homogenous. We may suggest that the critical compression ratio is laid between 15% and 20%. This means that for SIMA and RAP processing of 7075 Al alloy, at least 20%±2% strain is needed. We may propose a possible explanation for this: the internal strain energy stored in the alloy with less than 20% compression ratio

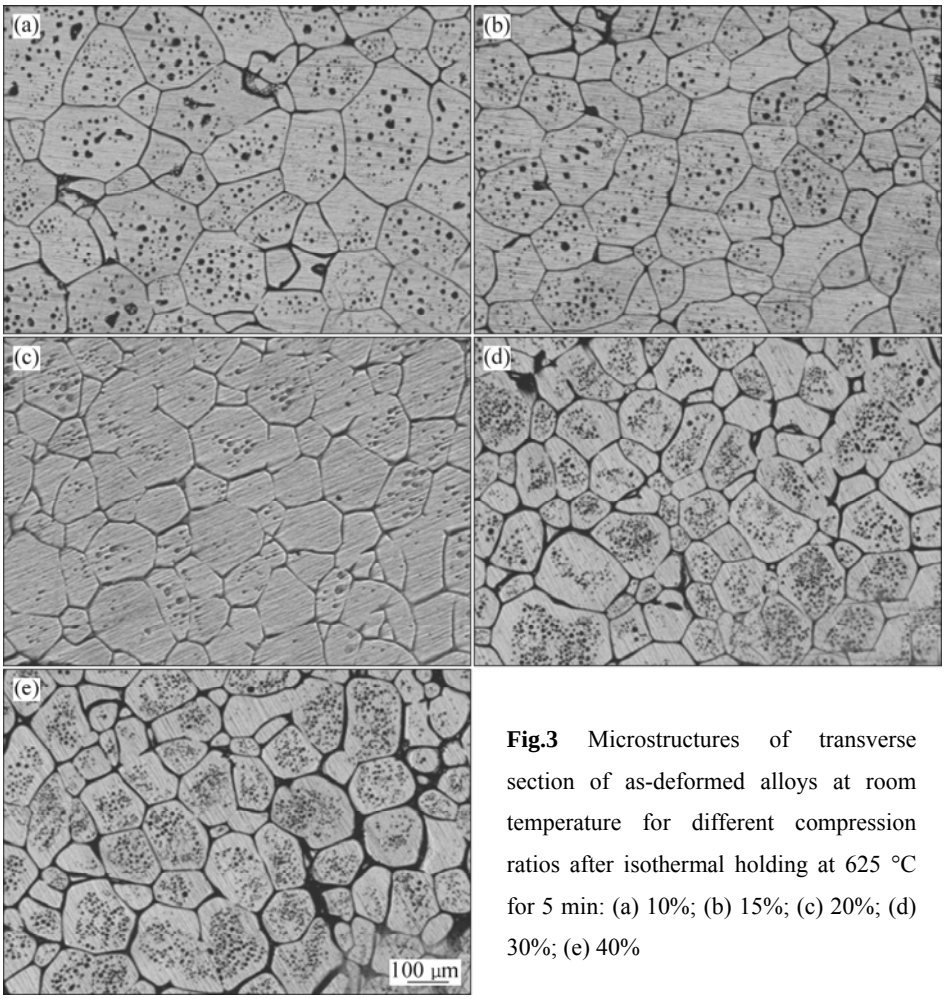

Fig.3 Microstructures of transverse section of as-deformed alloys at room temperature for different compression ratios after isothermal holding at 625 °C for 5 min: (a) 10%; (b) 15%; (c) 20%; (d) 30%; (e) 40%

is relatively low and cannot supply enough dislocation density in recrystallisation phenomena inside grains to induce subgrain boundaries with high energy, so breaking up mechanisms may be not effectively active. As shown in Figs.3(d) and (e), through the inducement of enough strain, the microstructures of the samples after isothermal holding consisted of homogeneous, globular solid particles surrounded by liquid film, which were suitable for semi-solid processing[2].

The general tendency, that is, a reduction in globular average grain size with an increase in compressive ratio of the alloys, at holding temperatures of 625, 620 and 610 °C is illustrated in Fig.4.

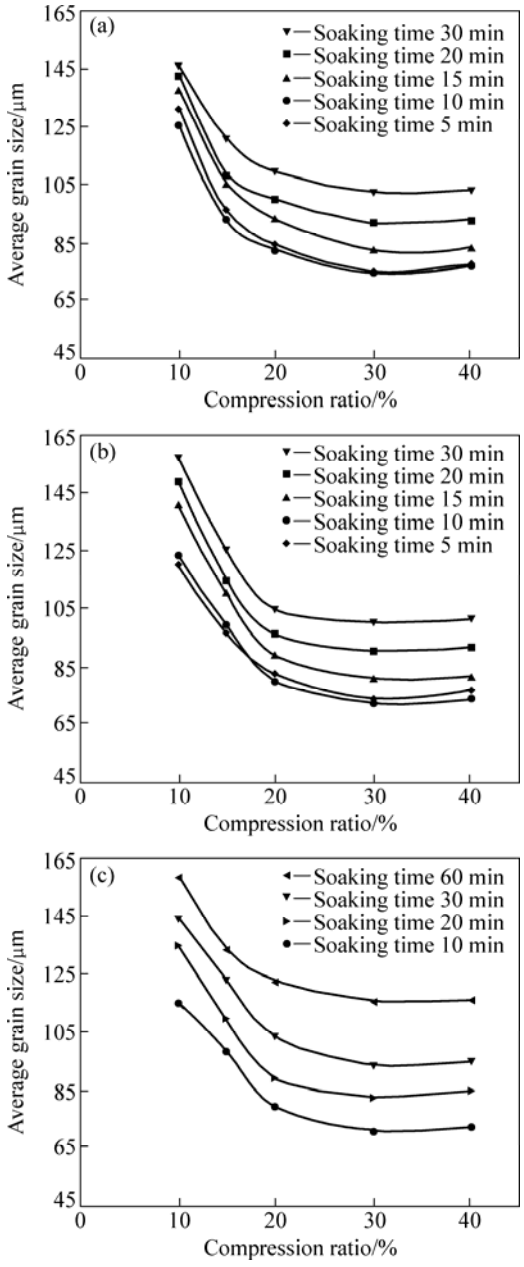

Fig.4 Variation in average grain size by applying different compression ratios and soaking times at different holding temperatures: (a) 625 °C; (b) 620 °C; (c) 610 °C

The results show that a precipitous decreasing characteristic in the average grain size for the 7075 Al alloy with the compressive ratio below 20% is depicted on the left region of the curve in Fig.4. An increase in the compressive ratio from 20% to 30% leads to a gentle reduction of average grain size of grains in the semisolid 7075 Al alloys, as illustrated by the middle region in Fig.4. For the right region of the curve in Fig.4, although the compressive ratio of the 7075Al alloy is increased from 30% to 40%, no significant reduction is observed on the average grain size of grains in the semisolid 7075 Al alloy. The main reason for precipitous decrease in average grain size might be that the deformation causes the strain energy to rapidly accumulate and abundantly store in the compressed alloy to get the critical point. By meeting the critical point in compression ratio, the accumulating rate of the strain energy is descended by degrees in the compressed alloys, which possibly weakens the effect of recrystallisation on the evolution of globular grains in the semisolid microstructure (between 20% and 30% of compression ratios). As the results show that the increase in compression ratio from 30% to 40% does not have any significant effect on the average grain size of alloy in the semi-solid state, we may propose two possible explanations for this.

1) As discussed, by increasing the compression ratio, we may expect that breaking up mechanism is active in sample with 40% compression ratio and recrystallisation has occurred, and then during soaking time grain growth and agglomeration have caused the same average grain size in comparison with the sample with 30% compressive ratio.

2) Considering the situation between 20% and 30% of compression ratios, it seems that the effect of compression (deformation) on the evaluation of microstructure is weakened and the stored strain energy has reached a peak value and may not exceed in the microstructure easily and more than the peak value, so the increase of the strain energy stored in the 7075 Al alloy is relatively limited.

To consider the probability of the two explanations, we will study the Fig.5 which shows the microstructures of as-deformed alloys with 30% and 40% compression ratios after isothermal holding at 620 °C for 5 min. For both of compression ratios, two sample observations are shown. Elongated grains in samples are observed and some cases are shown by arrows. As we have suggested that the main mechanism in breaking up the microstructure is recrystallization, these results show that during soaking time, recrystallisation has not occurred completely and liquid has not fully penetrated into subgrains. So, it seems that the explanation 1 is not correct, because according to the observation at 620 °C, both 30% and 40% compression ratios may have the

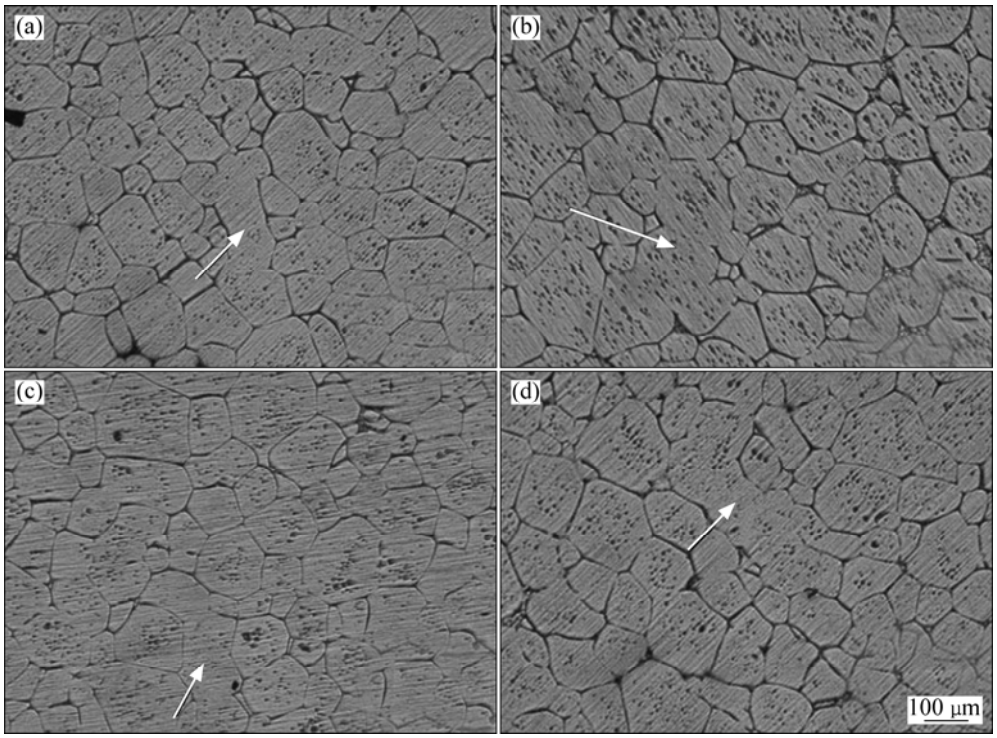

Fig.5 Microstructures of transverse section of as-deformed alloys at room temperature for different compression ratios after isothermal holding at 620 °C for 5 min: (a, b) 30%; (c, d) 40%

same effects on microstructure, and there are same elongated grains and almost same average grain size. It seems probable that the explanation 2 is correct. By increasing compression ratio, vacancies, lattice defect and dislocation (which form strain energy) may be neutralized, for example, two dislocations with opposite Burger vector will neutralize each other.

3.3 Microstructural evolution during partial melting

Fig.6 shows the microstructural evolution of a typical sample with 30% compression ratio during isothermal holding in the semisolid state at 620 and 625 °C. As soon as the deformed microstructure disintegrates into smaller grains parallel with liquid penetration and possible grain rearrangements, grain spherodization and coarsening (growth) mechanisms are active.

The probability of finding two neighboring grains with low energy grain boundary in Al alloys has been studied[19−20]. It is concluded that in a collection of touching grains with random orientations, the probability of finding four or more grains that are connected in a row with low energy grain boundaries to form agglomerate is small. Also in SIMA alloys, the final equiaxed microstructure is the result of fragmentation of a heavily deformed initial dendritic microstructure by liquid penetration at incipient melting in the high-energy grain boundaries formed in the alloy during the process. Therefore, it is expected that no extensive agglomerates are formed in SIMA alloys. Our experimental observations, as shown in Fig.6, support these arguments: the microstructure exhibits a uniform dispersion of solid grains in a liquid matrix specially at little soaking time and the presence of a weak skeleton at medium liquid contents. With the prolonged soaking time, the presence of smaller isolated grains and large agglomerates is observed. It is evident from Fig.3 that at the same time, as deformed microstructures are fragmented, grain coalescence may occur between newly formed grains.

The results show that SIMA microstructure does not require long soaking time in order to reach the degree of spheroidization which has a significant impact on the resistance to flow. And also the soaking time for SIMA should be minimal enough to ensure thermal equilibrium and the presence of a uniform distribution of liquid.

Fig.7 shows the microstructural evolution of a typical sample with 30% compression ratio during isothermal holding in the semisolid state at 610 °C. At this temperature, the liquid fraction is low and we may expect that the coalescence is the dominated mechanism for growth during heating. As shown in micrographs by arrows, many grain boundaries disappear, and we may expect that the rate of grain growth is high and the growth coefficient is large.

The intragranular liquid droplets present in a large number of the solid particles, appear to coarsen with time, reducing the number and increasing the average size.

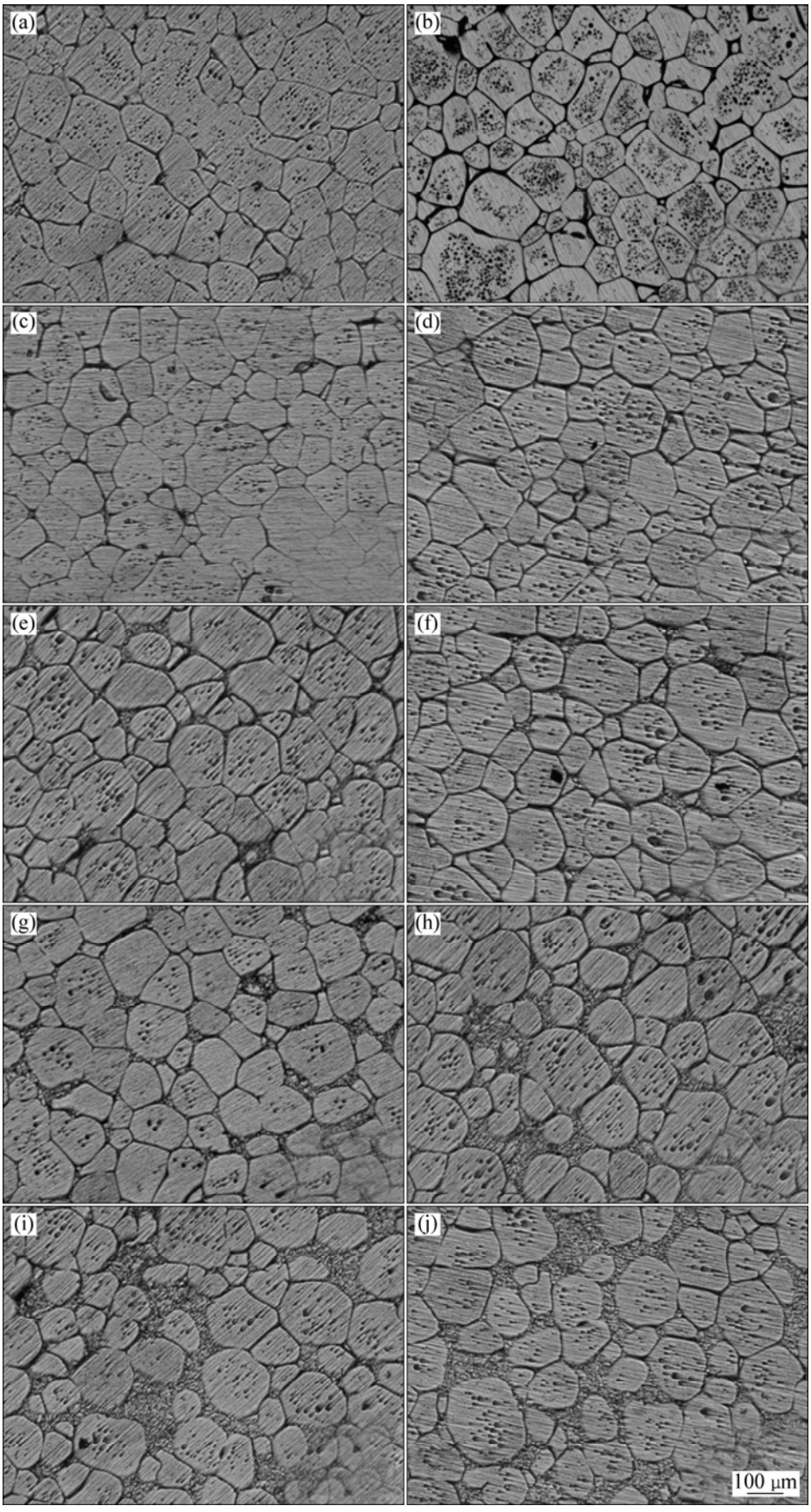

Fig.6 Microstructures of transverse section of deformed 7075 Al alloys with 30% compression ratio isothermally held for 5 min (a), 10 min (c), 15 min (g), 20 min (e) and 30 min (i) at 620 °C and 5 min (b), 10 min (d), 15 min (f), 20 min (h) and 30 min (j) at 625 °C

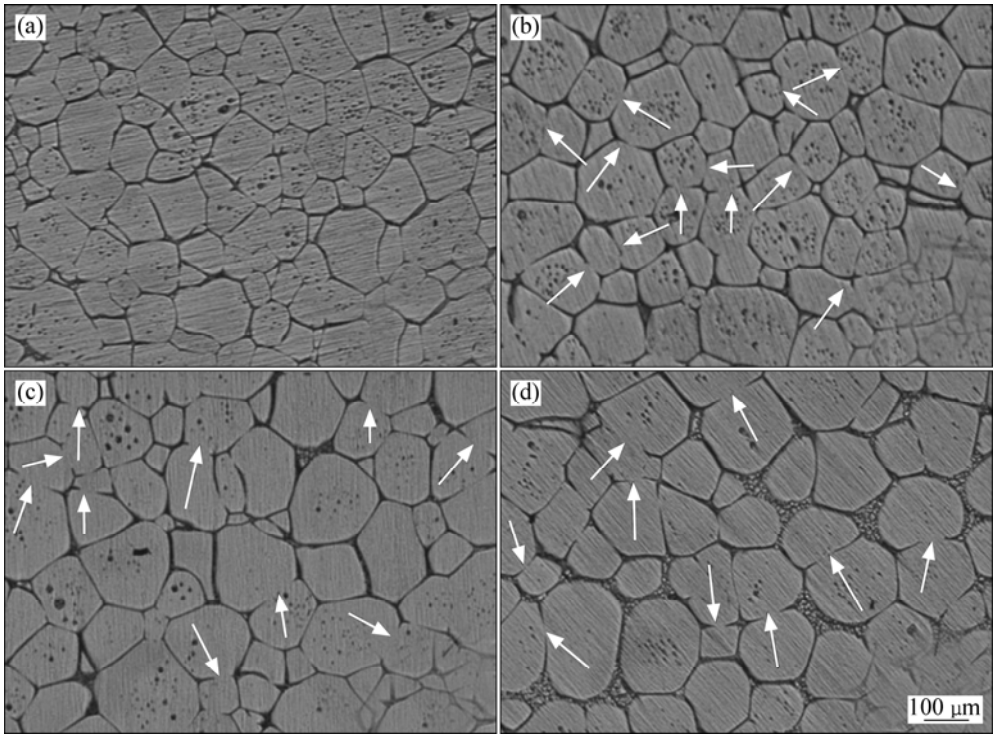

Fig.7 Microstructures of transverse section of sample with 30% compression ratio after isothermal holding at 610 °C for different holding times: (a) 10 min; (b) 20 min; (c) 30 min; (d) 60 min

These intragranular liquid droplets mainly originate from the internal inhomogeneity of the primary solid, which is caused by chemical segregation. With increasing holding time, some contiguous intragranular liquid droplets gradually merge into some big intragranular liquid droplets by coalescence. On the other hand, the number of small intragranular droplets also decreases by migration to some huge liquid intragranular droplets by diffusion through the solid phase (Ostwald ripening mechanism). Subsequently, these "new" intragranular liquid droplets become round in order to decrease the interfacial energy between solid and liquid phase. Finally, with long time it is expected, and it has been demonstrated elsewhere[17] that the amount of entrapped liquid decreases by migration to the liquid matrix by diffusion through the solid phase driven by the minimization of solid/liquid interface within the grain, which provides that no further coalescence occurs, as clearly demonstrated in Figs.7(a)−(d) .

3.4 As-deformed 7075 Al alloy coarsening kinetics

For many diffusion-controlled coarsening systems, including solid/liquid mixtures, coarsening kinetics can be described by the following equation:

$$D^n - D_0^n = Kt \tag{1}$$

where D and D_0 are the final and initial grain sizes, respectively; t is the isothermal holding time; K is a coarsening rate constant; n is the power exponent.

It is generally believed that n is 3 for volume diffusion-controlled coarsening, n is 4 for grain boundary diffusion-controlled coarsening, and n is 2 for interfacial reaction-controlled coarsening[21]. Many studies investigating solid/liquid coarsening of metals in the semi-solid state generally reported an exponent of n=3[12, 22]. Also K is in the form of[23]

$$K = \frac{8TD_{\mathrm{L}}\sigma}{9m_{\mathrm{L}}s_{\mathrm{f}}C_{\mathrm{L}}(k-1)} \tag{2}$$

where D_{L} is the diffusion coefficient of the solid in the liquid matrix; T is the coarsening temperature in absolute scale; C_{L} and k are the liquid composition and the partition ratio, respectively; s_{f} is the molar entropy of fusion; and R is the gas constant.

To calculate the coarsening rate constants, in the present study, a power law was used to fit the experimental data for grain coarsening. Fig.8 shows the evolution of the cube of the average globule diameter D^3 as a function of isothermal soaking time in the semi-solid state for 7075 Al alloy with 30% compression ratio at 610, 620 and 625 °C. Al alloys show generally high K (>600 $\mu m^3 \cdot s^{-1}$) in casting Al alloys and generally low K (<600 $\mu m^3 \cdot s^{-1}$) in wrought alloys[24]. The values of coarsening rate constant K from this work and also from Ref.[24] are summarized in Table 2.

At holding temperatures of 620 and 625 °C, the average grain size at initial holding time (300−600 s) is

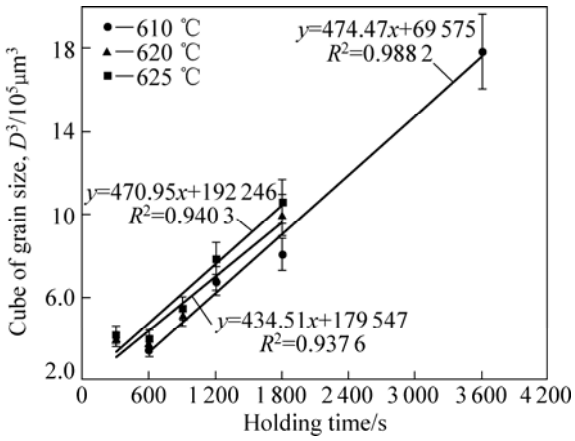

Fig.8 Evolution of average globule diameter D as function of isothermal holding time at 610−625 °C in semisolid state (Lines represent evolution according to $D^3=D_0^3+Kt$ and R^2 is regression coefficient)

Table 2 Values of coarsening rate constant K

Temperature/°C	K/(μm^3·s^{-1})	Source
625	471	Present work
620	434	Present work
610	474	Present work
620	500	Ref.[24]

almost constant (Fig.8). Mainly two different mechanisms have been identified to promote grain growth: grain coalescence and Ostwald ripening. The reason might be the result of Ostwald ripening mechanism. Ostwald ripening results from dissolution of material from high curvature interfaces and deposition to lower curvature interfaces. For a microstructure with variable curvature within every grain, Ostwald ripening occurs within each grain driven by the short diffusion distances, leading to a higher degree of spherodization. Only when every grain has a uniform curvature, will smaller grains be dissolved, leading to an increase in grain size. Liquid content plays an important role in kinetics of coalescence since it defines the number of solid necks between grains. It has been shown that the coalescence frequency is proportional to the number of adjacent grains. Therefore, coalescence is expected to occur at early stages of heating or in high fraction solid in the semi-solid regime where the number of necks per grain is relatively high and grains are discrete. But results show no significant change in average grain size at initial holding time. According to the results in Fig.5, it seems that with increasing holding time to 600 s, breaking up mechanism is in balance with coalescence mechanism; in other words, the average grain size does not change during holding time of 300−600 s because an elongated grain which disintegrates in breaking up processes may be replaced by an aggregate due to coalescence mechanism.

At higher fraction liquid, aggregates that have grown by coalescence do not melt but may lose contact with other aggregates. Similarly, the solid contact around each aggregate decreases, leading to extended diffusion fields necessary for rapid spherodization. Therefore, there is a time limit above which grain coalescence becomes too slow and Ostwald ripening becomes the dominant growth mechanism (1 200−1 800 s).

And also in an interval, the both mechanisms are active simultaneously. We may suggest that it can be 600−1 200 s because of precipitous increase in average grain size. We may conclude that Ostwald ripening and grain coalescence operate simultaneously and independently as soon as liquid is formed which is in common with what TZIMAS and ZAVALIANGOS[17] suggested. But clearly, it is expected that Ostwald ripening is dominant at longer time and at high volume fractions of liquid, while growth by coalescence by grain boundary migration is dominant at short time after liquid is formed at low volume fractions of liquid.

According to Table 2, the K value descends by decreasing temperature from 625 to 620 °C probably because of temperature (T) term. According to Dohetry theorem[22], the K value increases with fraction solid increasing. We may assume that according to the result of MANSON-WHITTON et al[25], the transition solid fraction value to consider the Dohetry theorem is not satisfied. The value for 620 °C is in common with other studies and the difference may result from alloying difference. But by decreasing temperature to 610 °C, the K value increases. In previous section and according to Fig.8, we may expect higher K value for this temperature because of a lot of necking in microstructure. Also, we may assume that the transition solid fraction may be satisfied for Dohetry theorem and by increasing solid fraction, the K value increases.

4 Conclusions

1) The descending trend in average diameter of the α(Al) grains in the semisolid microstructure as a function of deformation degree experiences three different stages, which respectively exhibits precipitous, gentle and constant characteristics. The main reason might be that the increase of the systemic strain energy gradually limited.

2) The microstructures of deformed alloy isothermally held in the semi-solid state consist of round solid grains surrounded by grain boundary liquid films. The intragranular liquid droplets are present in a large number of the solid particles, reducing the number and increasing the average size with time.

3) After the spheroidization is completed,

coarsening and agglomerating occur, and the spherical grains change into coarsened spherical grains.

4) A lower coarsening rate is observed for 620 °C (coarsening rate K=434 $\mu m^3 \cdot s^{-1}$) compared with for 610 °C (coarsening rate K=474 $\mu m^3 \cdot s^{-1}$) despite of the higher fraction liquid for the former.

References

[1] FLEMINGS M C. Behavior of metal alloys in semi-solid state [J]. Metal Tarns A, 1991, 22: 269−293.

[2] KIRKWOOD D H. Semi-solid metal processing [J]. International Material Reviews, 1994, 39: 173−189.

[3] FAN Z. Semisolid metal processing [J]. International Material Reviews, 2002, 47: 49−85.

[4] ATKINSON H V. Modelling the semisolid processing of metallic alloys [J]. Progress in Materials Science, 2005, 50: 341−412.

[5] ATKINSON H V, KAPARNOS P, KIRKWOOD D H. Alloy development for thixoforming [C]//Proc 6th International Conference on Semi-Solid Processing of Alloys and Composites, Torino, Italy, 2000: 443−450.

[6] Jİ S, FAN Z, BEVİS M J. Semi solid processing of engineering alloys by a twin screw rheomoulding process [J]. Materials Science and Engineering A, 2001, 229: 210−217.

[7] MEHRABİAN R, FLEMİNGS M C. Die castings of partially solidified alloys [J]. AFS Transactions, 1972, 80: 173−182.

[8] ASUKE F. Rheocasting method and apparatus. United States Patent 5865240 [P]. 1999.

[9] YOUNG K P, KYONKA C P, COURTOIS F. Fine grained metal composition. United States Patent 4415374 [P]. 1983.

[10] KİRKWOOD D H, SELLARS C M, ELİAS-BOYED L G. Thixotropic materials. European Patent 0305375 B1 [P]. 1992.

[11] ATKINSON H V, BURKE K, VANEETVELD G. Recrystallisation in the semi-solid state in 7075 aluminum alloy [J]. Material Science and Engineering A, 2008, 490: 266−276.

[12] CHAYONG S, ATKINSON H V, KAPRANOS P. Thixoforming 7075 aluminum alloys [J]. Material Science and Engineering A, 2005, 390: 3−12.

[13] CHAYONG S, ATKINSON H V, KAPRANOS P. Multistep induction heating regimes for thixoforming 7075 aluminum alloy [J]. Materials Science and Technology, 2004: 20(4): 490−496.

[14] CHOU H N, GOVENDER G, IVANCHEV L. Opportunities and challenges for use of SSM forming in the aerospace industry [C]//9th International Conference on Semi-Solid Processing of Alloys and Composites. Busan, South Korea, 2006.

[15] VANEETVELD G, RASSILI A, PIERRET J C. Improvement in thixoforging of 7075 aluminium alloys at high solid fraction [C]//10th International Conference on Semi-Solid Processing of Alloys and Composites, Aachen, Germany, 2008.

[16] VANEETVELD G, RASSİLİ A, PİERRET J C, LECOMTE-BECKERS J. Extrusion tests of 7075 aluminium alloy at high solid fraction [J]. Int J Mater Form, 2008(Suppl.1): 1019−1022.

[17] TZIMAS E, ZAVALIANGOS A. Evaluation of volume fraction of solid in alloys formed by semisolid processing[J]. Journal of Materials Science, 2000, 35: 5319−5329.

[18] DOHERTY R D, LEE H I, FEEST E A. Microstructure of stir-cast metals [J]. Materials Science and Engineering, 1984, 65: 181−189.

[19] WAN G, SAHM P R. Particle characteristics and coarsening mechanisms in semisolid processing [C]//BROWN S B, FLEMİNGS M C. 2nd International Conference on the Semi-Solid Processing of Alloys and Composites, MIT. Cambridge, 1992.

[20] WARRINGTON D H, BOON M. Ordered structures in random grain boundaries: Some geometrical probabilities [J]. Acta Metall, 1975, 23: 599.

[21] FAN Z, LİU G. Solidification behavior of AZ91D alloy under intensive forced convection in the RDC process [J]. Acta Materialia, 2005, 5: 4345−4357.

[22] ANNAVARAPU S, DOHERTY R D. Inhibited coarsening of solid-liquid microstructures in spray casting at high volume fractions of solid [J]. Acta Metallurgica et Materialia, 1995, 43: 3207−3230.

[23] HARDY S C, VOORHEES P W. Ostwald ripening in a system with a high volume fraction of coarsening phase [J]. Metallurgical Transactions A, 1988: 2713−2719.

[24] ATKINSON H V, LIU D. Microstructural coarsening of semi-solid aluminum alloys [J]. Material Science and Engineering, 2008: 439−446.

[25] MANSON-WHITTON D, STONE I C, JONES J R, GRANT P S, CANTOR B. Isothermal grain coarsening of spray formed alloys in the semi-solid state [J]. Acta Materialia, 2002, 50: 2517−2535.

(Edited by YANG Bing)